ELSEVIER

Nuclear Instruments and Methods in Physics Research A 490 (2002) 159–168

NUCLEAR INSTRUMENTS & METHODS IN PHYSICS RESEARCH Section A

www.elsevier.com/locate/nima

Tagging of isobars using energy loss and time-of-flight measurements

D. Shapira*,[1], T.A. Lewis, P.E. Mueller

Physics Division, Oak Ridge National Laboratory, P.O. Box 2008, Oak Ridge, TN 37831, USA

Received 3 May 2001; received in revised form 21 March 2002; accepted 28 March 2002

Abstract

The technique for tagging isobars in a mixed beam using differences in energy lost in an absorber by different isobars has been tested. As expected, isobar separation does improve by allowing more energy loss (thicker absorbers), but such gains could be realized only after achieving good absorber homogeneity. For heavy ions accelerated to low and moderate energies (<30 MeV/A), we found that when homogenous absorbers are used, the largest impediment to achieving good isobar separation rests with uncertainties in energy caused by straggling in the absorber. Measurements of beam energy loss and energy spread were shown to come close to predicted values when accounting for both collisional and charge-exchange contributions to the calculated energy straggling. Reliable prediction of energy straggling then allowed us to study the efficacy of this method for isobar separation when applied to different mass ranges and beam energies. Time-of-flight was used to measure energy loss since this method allows handling of counting rates in excess of 1 MHz and the demands on timing detector resolution and length of flight path were moderate for all cases under study here. Partial separation in a most difficult case, an analyzed beam of $A = 132$ isobars at energies near 3 MeV/A has been demonstrated. The time-of-flight information can be added to the data stream for events of interest, as an additional parameter (tag) to the online data stream. Such event-by-event tagging enables one to study the effect of difference in isobaric mixture in the beam on the reaction outcome even when isobar separation is not complete. © 2002 Published by Elsevier Science B.V.

PACS: 29.27 Eg; 29.30 −h; 29.40 Gx

Keywords: Radioactive ion beams; Isobar tagging; Time-of-flight

1. Introduction

In general, one may expect isobaric contaminants to be present at some level in the beams delivered at radioactive ion beam (RIB) facilities. This may be due to the inherent method of beam delivery, for example, a mixture of beams with similar mass-to-charge ratios from a fragmentation source or isobars that escape separation in beams delivered from an Isotope Separation On Line (ISOL) source. In the next generation of RIB facilities, where deceleration and re-acceleration of RIBs with very short lifetimes (1 ms) is contemplated, decay-in-flight may also introduce

*Corresponding author. Tel.: +1-865-576-2648; fax: +1-865-574-1268.

E-mail address: shapira@mail.phy.ornl.gov (D. Shapira).

[1] Managed by UT-Battelle, LLC for the U.S. Department of Energy under contract DE-AC05-00OR22725.

0168-9002/02/$ - see front matter © 2002 Published by Elsevier Science B.V.
PII: S0168-9002(02)01058-6

significant amounts of isobaric contamination. Since isobars are very close in mass, their separation is not an easy task.

When isobar masses are separated by a small fraction of their total mass ($\leqslant 1/20\,000$), separation via momentum (magnetic spectrograph) or time-of-flight (TOF) measurements is extremely difficult. Isobars are most easily separated by exploiting their difference in nuclear charge (z). If isobars with the highest nuclear charge need to be isolated, full stripping of the beam of ions can be combined with magnetic analysis (mostly low mass and high energy) to remove lower z contaminants. In cases where beam intensity is less than a few thousand ions/s, energy loss in an ionization chamber can be used to measure the nuclear charge and tag the isobars. At higher beam intensities, the combination of a passive absorber and a TOF measurement can be used to measure energy loss and determine the nuclear charge. The TOF detectors can handle rates up to several MHz ($<10^7$/s). This method can be applied with different degrees of success depending on the energy and mass of the beams under investigation. It is particularly difficult for heavy and medium mass nuclei at energies below 6 MeV/A such as are contemplated for many ISOL-based RIB facilities planned or under construction world wide. In this paper we show that thin absorber foils are practically useless as energy degraders for this mass and energy regime. By using a specially designed gas-filled cell as absorber material, we were able to keep absorber inhomogeneity below 0.5%. Under such conditions, we can predict the spread in beam energy as a function of nuclear charge, mass, energy, and energy loss with remarkable accuracy. In this paper we compare predictions of resolving power with this method to measurements in several cases. Limits to this method's applicability are discussed and a successful application of this method to the most difficult task of tagging $A = 132$ isobars is demonstrated.

2. Description of method

Ions, with kinetic energies below 1 GeV/nucleon, passing through an absorber lose energy mostly through repeated ionization of the medium's atoms. This electronic energy loss is approximated by the Bethe–Bloch formula. Projectile dependence in this formula is through the mass, the inverse of the kinetic energy, and the square of the nuclear charge (z) [1]. Therefore, the fractional difference in energy loss suffered by two neighboring isobars moving at the same velocity is given approximately by $2/z$. For the case of $z = 28$ neighboring isobars (^{56}Ni and ^{56}Co), this amounts to about 7%. If the energy loss suffered by the ions passing the same absorber is a significant fraction of the ion's total energy ($0.1 \leqslant \Delta E/E \leqslant 0.5$), the difference in isobar energies as they emerge from the absorber will be significant and detectable ($0.007 \leqslant \Delta E/E \leqslant 0.035$, correspondingly). The situation, though, is complicated due to spread in the ion's energy as it passes the absorber. The spread is caused by energy loss straggling and by inhomogeneities in absorber thickness. The difference in energy losses suffered by neighboring isobars, which varies linearly with energy loss, will eventually become larger than the spread caused by energy straggling, which is proportional to the square root of the energy loss. When planning to apply this method, one needs reliable estimates for energy loss and energy straggling of the isobars passing the absorber medium of choice. Energy loss estimates presented here, made with the code SRIM [2], were shown to be reliable in all our tests. The energy straggling predicted by SRIM, however, turned out to be much smaller than the values we measured for all particles heavier than $A = 4$. A recipe to calculate energy straggling for heavy ions that includes contributions from collisional recoil (σ_{coll}) and ion-charge fluctuations (σ^2_{ch}) provided more accurate results [3]. These values for heavy nuclei are generally higher than predictions by SRIM which apparently include only the collisional term (σ_{coll})

$$\sigma^2 = \sigma^2_{\mathrm{coll}} + \sigma^2_{\mathrm{ch}} \tag{1}$$

where the collision term σ^2_{coll} is

$$\sigma^2_{\mathrm{coll}} = \Omega Q^2_{\mathrm{eff}} \left[1 + \frac{T}{aM_{\mathrm{u}}} + \frac{1}{2}\left(\frac{T}{aM_{\mathrm{u}}}\right)^2 \right] \tag{2}$$

and the charge fluctuation term σ_{ch}^2 is

$$\sigma_{ch}^2 = \Omega Q_{eff}^2 \frac{C}{2}\left(1 - \frac{Q_{eff}}{z}\right) Q_{eff} \quad (3)$$

where Ω embodies the dependence on the absorber medium

$$\Omega = D\frac{Z}{A} m_e t \rho. \quad (4)$$

The effective charge of the ion passing through the absorber, Q_{eff}, is a function of the kinetic energy and the nuclear charge of the incident ion and is given by a semi-empirical formula [3]

$$Q_{eff} = z[1 - (1.034 - 0.1777e^{-0.08114z})e^{-\chi}]. \quad (5)$$

The dimensionless quantity χ depends on the ion's kinetic energy and is defined by

$$\chi = 121.4139\frac{\beta}{z^{2/3}} + 0.0378\sin\left(190.7165\frac{\beta}{z^{2/3}}\right). \quad (6)$$

In the formulae above

$a =$ projectile mass number,
$z =$ projectile nuclear charge number,
$T =$ kinetic energy of the projectile,
$A =$ atomic mass number of absorber medium,
$Z =$ atomic charge number of absorber medium,
$M_u =$ atomic mass unit equivalent energy (938 MeV),
$m_e =$ electron mass equivalent energy (0.511 MeV),
$\rho =$ absorber density in mg/cm^3,
$t =$ absorber thickness in cm,
$\beta =$ projectile velocity divided by the velocity of light,
$D =$ 3.07×10^{-3} MeV cm^2/mg,
$C =$ 2.5; semi-empirical parameter derived from straggling data.

For the proposed method of isobar separation to succeed, the difference in energy loss between two neighboring isobars must exceed the spread in their final measured energy. In this paper the SRIM code [2] will be used for calculating energy loss and multiple scattering and Eqs. (2)–(6) to calculate energy spread (FWHM). This procedure holds for all the values quoted in tables and displayed in graphs.

3. Measuring energy loss and energy spread for heavy ions passing through absorbers

Before attempting to tag isobars in a mixed radioactive beam, we evaluated the assumptions made for beam energy spread in the absorber. Reliable estimates of beam energy spread as a function of beam energy loss are most critical for planning isobar separation with this technique. When considering the use of this technique for beam tagging, we also need to consider the loss in beam intensity due to multiple scattering in the absorber. The beam can spread to a very large size if it is not refocused. Requirements that will render this method for isobar separation viable are as follows:

- The isobars must experience substantial energy loss (absorber material and thickness).
- The uncertainty in post-absorber beam energy must be minimized (absorber homogeneity).
- The TOF measurements must be optimized (instrumentation).
- The beam transmission must be optimized (beam focussing).

A test beamline with two timing detectors, and one quadrupole doublet and two magnetic steerers between them, was used to measure the TOF of beam particles. Fig. 1 shows a schematic layout of the beamline that we used. It shows the location of a mechanism for inserting different absorbers at a close distance following the first timing detector. Two timing detectors (see Ref. [8]) were built and

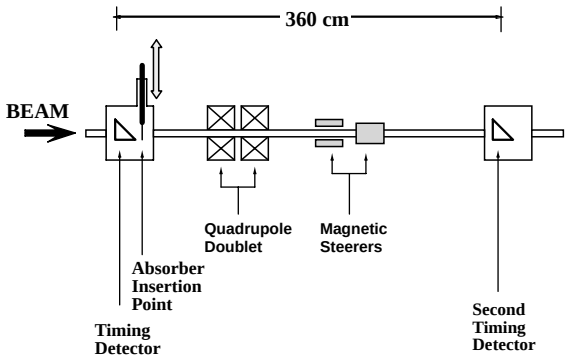

Fig. 1. Beamline setup for studying isobar tagging.

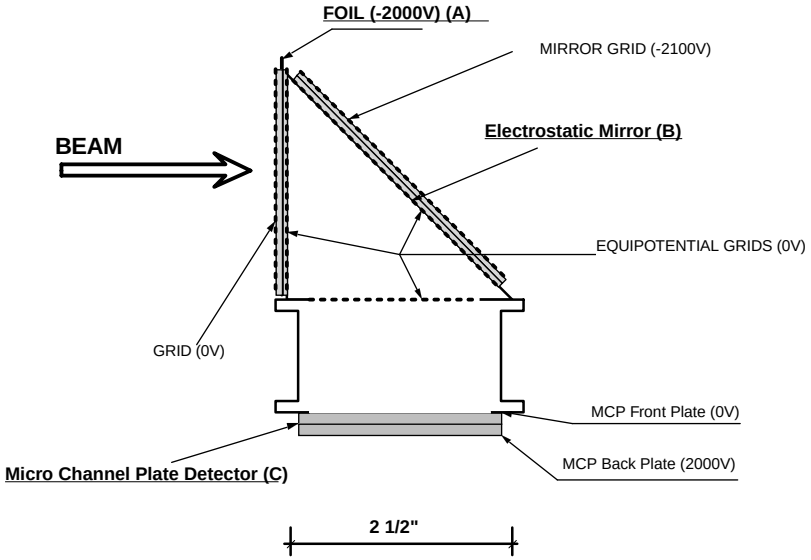

Fig. 2. Components of the timing detector—a sketch.

tested and are shown in Fig. 2. The beam hits a thin carbon foil (10 μg/cm^2) and continues, almost unscathed, past the detector. The electrons ejected from the foil, upon beam passage, are accelerated toward the slanted electrostatic mirror (B) and are reflected toward a micro-channel plate detector (C) where they are multiplied to produce a detectable current.

When mounted in close proximity in order to minimize the spread in flight time, overall time resolution with 110 MeV ^{32}S beam was about 120 ps. Simulations we present later indicate that our final energy resolution is limited, in most cases, by the spread in ion energy due to straggling in the thick absorber.

3.1. *First test with* ^{58}Ni *beam*

We plan to measure fusion cross-sections for ^{56}Ni with different targets at near and sub-barrier energies. In these measurements, the target is bombarded with ^{56}Ni beams at several energies near the barrier and cross-section for evaporation-residue and fission-fragment production are measured. The beam will be produced at the Holifield Radioactive Ion Beam Facility (HRIBF) at Oak Ridge National Laboratory (ORNL) with a batch mode ion source where ^{56}Ni is sputtered from a ^{58}Ni target that has been previously bombarded with an intense proton beam for several hours [4]. This ion source will also produce copious amounts of ^{56}Co that will be hard to separate from ^{56}Ni. As a result, a mixed beam of ^{56}Ni and ^{56}Co will reach the target. It will be impossible without tagging to determine whether detected evaporation residues or fission products result from collisions between ^{56}Co or ^{56}Ni with the target nucleus. If we were able to tag the beam before it reaches the target and provide this information every time a fusion or fission product is detected, we could determine whether the process originated from reactions with ^{56}Ni or ^{56}Co. The expected rates of accelerated ^{56}Ni beam at HRIBF is below 10^6/s. Such rates, when combined with 5- to 6-fold higher ^{56}Co yield, can be handled by the proposed tagging method.

Several TOF measurements for 235 MeV ^{58}Ni test beam were made with the two timing detectors and several different absorber foil combinations inserted into the beamline. The absorber foils we used were made of Mylar and polypropylene (with thickness ranging between 1 and 15 μm). The results of several such measurements are shown in Fig. 3. Plotted are the measured energy spread

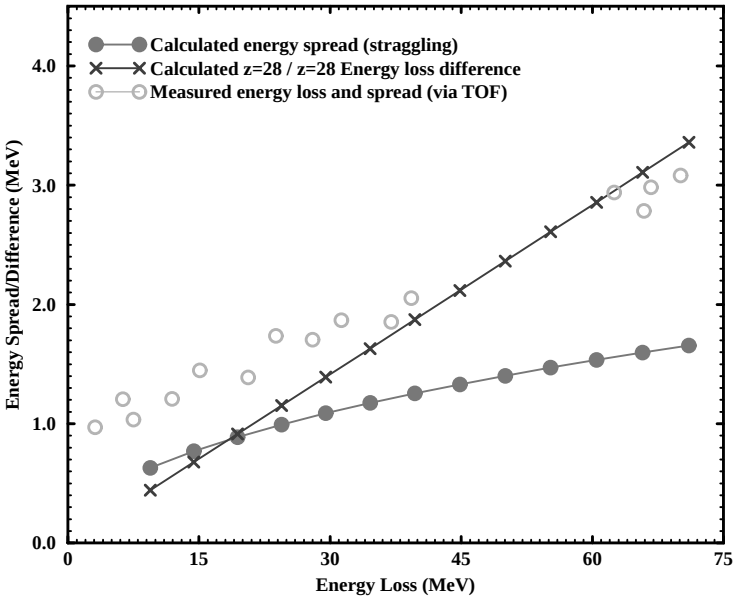

Fig. 3. Measured and calculated energy spread for 235 MeV ^{58}Ni passing through different absorber foil combinations. Also shown is the predicted difference in energy loss suffered by ^{58}Ni and ^{58}Co.

as a function of the total energy loss as derived from the measured TOF data. Also shown for comparison are the calculated values for energy spread. The same figure also displays differences in energy calculated using SRIM for 235 MeV ^{58}Ni and ^{58}Co ions that passed through an absorber as a function of the energy loss that would be suffered by ^{58}Ni. We can make two observations. First, the calculated energy spread due to straggling is smaller than the values that we measured. Second, the measured dependence of energy spread on energy loss is linear and does not vary as the square root of the energy loss as expected. The slope indicates that an average of about 2% inhomogeneity in the foil thickness could account for most of the observed energy spread. In the case shown here, even a 75 MeV energy loss (30% of the total energy) would not be sufficient to accomplish isobar separation. We have found this type of behavior in several different batches of Mylar and polypropylene foils. It became clear that in order to learn about the contribution of straggling to the spread in beam energy after passing an absorber, one first has to control the contributions from absorber inhomogeneity.

3.2. *Building a homogeneous absorber—second test with* ^{58}Ni

We have decided to use a gas cell as a means to achieve a high degree of uniformity in the beam energy degrader thickness. A 7 cm long cylindrical gas cell with thin (0.9 μm) entrance and exit windows was built. The absorber gas chosen, isobutane (C_4H_{10}), has relatively low nuclear charges but is a relatively heavy molecule. This choice provides an efficient absorber and also minimizes angular spread of the beam due to multiple scattering. To further control inhomogeneity, the gas cell had to be designed so that window bowing would be kept to a minimum and that the small but inevitable gas leaks through the thin window foils would not cause large pressure fluctuations. The cell has a $\frac{3}{4}$ in. diameter 0.9 μm thick Mylar window with a support grid made of tightly strung Kevlar strings mounted flush against the window to prevent bowing. We have also added an 8 liter ballast volume in parallel with the cell's volume (<0.05 liter) to minimize pressure fluctuations. Preventing window bowing and pressure fluctuations proved critical in keeping inhomogeneities below 0.5%.

We then made similar measurements with 270 MeV ^{58}Ni at rates near 19^6/s, this time using different amounts of gas in the cell to vary the amount of energy loss in the absorber. The results are shown in Fig. 4. This time the measured energy spread is much closer to the calculated values. More important, it shows the same trend in both calculated and measured energy spread, both increase as the square root of the magnitude of the energy loss. The zero offset (about 0.92 MeV at zero energy loss) is attributed to the instrumental TOF resolution that was close to 210 ps for this setup. From the data presented in Fig. 4, it is clear that allowing for energy loss of 30% of the total energy would suffice to separate ^{56}Ni and ^{56}Co when the need arises. Table 1 lists the relevant quantities after allowing for 90 MeV energy loss of ^{58}Ni in the absorber.

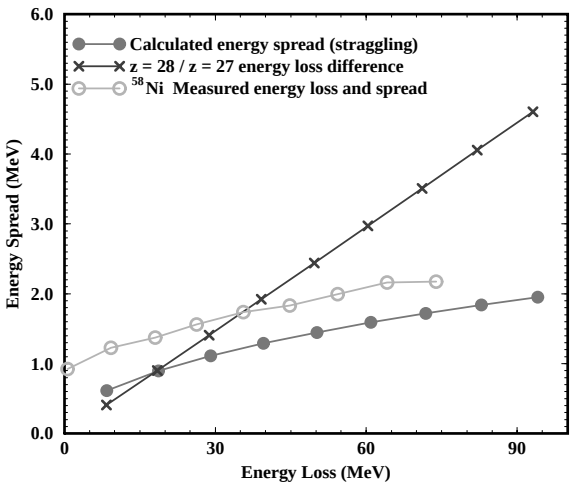

Fig. 4. Measured and calculated energy spread for 270 MeV ^{58}Ni passing through the gas cell and the anticipated separation for $z = 27$ and 28 isobars.

3.3. Simulation of expected TOF separation

The actual tagging in our experiments is performed with TOF measurements. The measured TOF of the particle exiting the absorber and transmission efficiency are affected by several factors. Among these are detectors' timing resolution, deterioration in beam quality after passing through the absorber, variations in ion trajectories between detector and the layout of focussing elements in the beamline. In two typical cases, shown in Table 1, energy straggling produces some 2–3% spread in energy. This spread in energy/TOF dwarfs, for the range of cases considered in this study, the effect of uncertainties in detector resolution or flight path differences in straight beamline sections.

We have decided to employ simulations in studying the effect of all these variables. In our simulation, beam particles are generated one at a time, by sampling from characteristic distributions expected of a beam exiting the energy degrading absorber (object). The particles are then propagated to the second timing detector (image) where their hit pattern and flight time are recorded. The incident beam position, and energy, charge state, and angle of emission following passage through the absorber are sampled. Particle propagation, once its exit parameters from the absorber have been set, is determined by the electro-magnetic elements in the beamline. To calculate the ion trajectories, an output MAP from the charged particle optics code COSY [5] is used. The MAP is calculated by COSY and determines the transfer function between object and image that takes into account all the magnetic and electrostatic elements between the two points. We first calculate the transfer MAP for particles having the correct initial spread in position and angle, but with only

Table 1
Degradation in beam quality for ions passing through an absorber material

Isobar Mass	E-Beam (MeV)	E-Loss (MeV)	E-Straggling (MeV)	E-Difference (MeV)	Q_{eff}	Multiple Scattering (°)
$A = 58$	270	90	2.00	4.50	21.7	0.43
$A = 17$	40	20	0.37	3.68	7.1	0.68

one energy and charge state set to the average charge state as listed for ^{58}Ni in Table 1. We use COSY to search for settings that would optimize transmission from a finite object (the exit of the absorber) to an image (the second detector) by keeping the image as small as possible and the magnification close to -1. Once the best solution is found, we use the MAP given by COSY to propagate all the particles in our simulation incorporating the actual spread in charge state and beam energy and detector's intrinsic time resolution. The simulation program generates a two-dimensional hit pattern at the image plane as well as a TOF spectrum.

Fig. 5 shows the TOF spectrum that can be expected for a 1:1 mixture of 270 MeV ^{56}Ni and ^{56}Co allowing for 90 MeV energy loss in the absorber (see Fig. 4). The degree of separation expected is shown in Fig. 5. It shows the TOF spectra for ^{56}Ni alone and for the mix of ^{56}Ni and ^{56}Co. The detector resolution assumed in our simulation was about 310 ps and is much lower than the 2.8 ns FWHM seen in Fig. 5. Simulations under different conditions have shown that the main culprit causing the observed spread in TOF is energy straggling in the absorber. The remedy is to allow more energy loss in the absorber that will bring about an increase in the energy difference between ^{56}Ni and ^{56}Co. The expected increase in energy straggling, should occur at a lower rate. The same simulation also showed that the transmission from the first timing detector to the second is better than 50% for beam sizes varying from 3 to 10 mm in diameter (allowing no increase in beam diameter size at image plane). We define the transmission efficiency as the ratio of the number of hits at the image plane that fall within the area bound by the object size to the total number of particles launched. With this definition the transmission without the beam focussing elements would have been about 0.2% or 2.0% for beam size diameters of 2 and 10 mm, respectively.

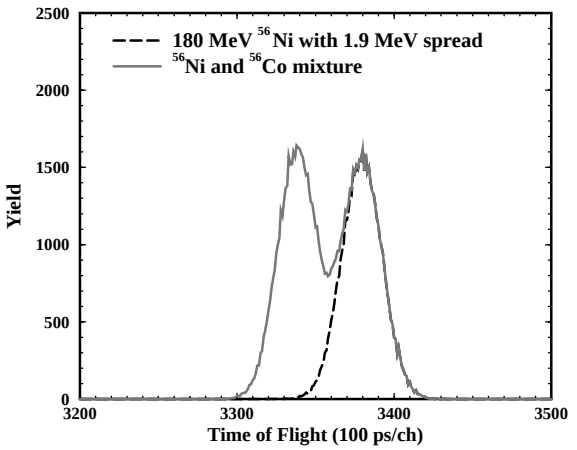

Fig. 5. Simulated TOF spectra for ^{56}Ni and a mixture of ^{56}Ni and ^{56}Co.

3.4. Separation of ^{17}F and ^{17}O

Nuclear reactions between light ($A<40$) radioactive beams and light targets are of interest to nuclear astrophysicists because they may represent nuclear processes taking place in the hot interiors of exploding stars. Several of these studies were conducted at HRIBF with radioactive ^{17}F beams at energies ranging between 15 and 33 MeV [6,7]. The RIB ion source produces ^{17}F along with a copious amount of ^{17}O. When coincidence detection of binary products is feasible, contributions from different beam species can be unfolded, but with low intensity radioactive beams this luxury is not always afforded. In thick target experiments [7], we made sure that only ^{17}F arrives at the experiment by stripping the ion beam at the end of the acceleration cycle and tuning the final analyzing magnet to allow only charge state 9^+ to go through, thus insuring complete rejection of ^{17}O. At 20 MeV ^{17}F, however, only 3% of the beam will be fully stripped, i.e., a 97% loss in beam intensity ensues. The method of isobar tagging discussed here could become an attractive alternative at such low energies.

Fig. 6 shows predictions of energy straggling for 40 MeV ^{17}F passing through the gas absorber, as a function of energy loss. Also shown is the difference in energy between ^{17}F and ^{17}O that had the same initial energy and passed through the same absorber. It is obvious from Fig. 6 that separation of ^{17}F and ^{17}O will be an easy task.

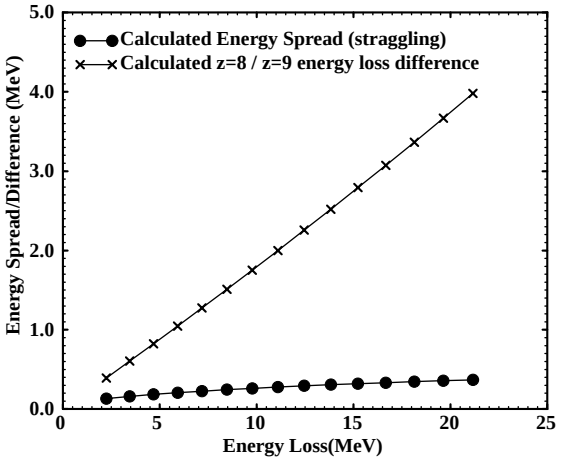

Fig. 6. Energy straggling for 40 MeV ^{17}F and difference in energy loss of nearest isobar ^{17}O as a function of total energy loss.

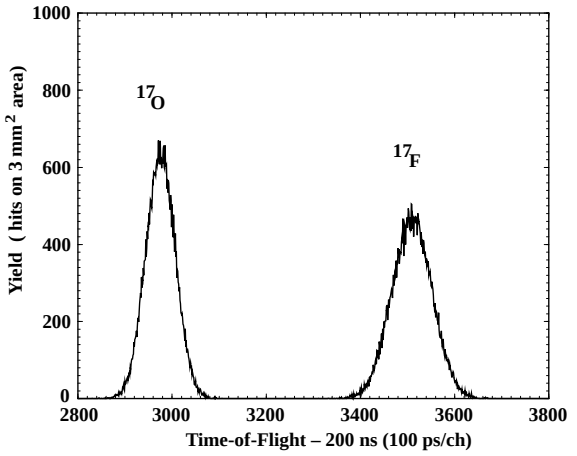

Fig. 7. Simulated TOF spectra for a 1:1 mixture containing ^{17}F and ^{17}O, initial energy 40 MeV, $\Delta E = 20$ MeV.

The simulated TOF spectrum for a 1:1 mixture of ^{17}F and ^{17}O is shown in Fig. 7. It shows that complete separation of 20 MeV ^{17}F is possible on an event-by-event basis achievable at combined rates of ^{17}O and ^{17}F below 10^7/s. The relevant quantities after allowing for approximately 20 MeV energy loss for the $A = 17$ mixture are listed in Table 1. The incident beam and object size, in this simulation, are bounded by a 3-mm diameter circle. The overall transmission predicted in our simulation, which incorporates fluctuations in beam energy, charge, and angular spread, is still near 50% (and higher if we allow larger image sizes). The main contribution to the predicted spread in TOF is from the 370 keV spread in the ion's energy due to energy straggling in the absorber.

Measurements presented in this section show that we can use SRIM [2], and formulae from GEANT [3] to make predictions about energy loss and energy spread for ions passing through an absorber medium quite reliably. This information combined with the detector system's time resolution and properties of the beamline allows us to predict the efficacy of using energy loss data to tag isobar mixtures in the beam. The next section shows the results from a case where this method was put through a most stringent test.

4. Isobar separation in a mass 132 mixture

The beam of mass $A = 132$ produced in the HRIBF fission source is known to contain a mixture of several isobars [9]. The beamline leading from the source to the post-accelerator is equipped with a large magnet designed to help with isobar separation. We tried the technique of energy-loss measurements to test if we can tag isobars in the accelerated beam. Such measurements could help us obtain immediate feedback on the effects of tuning the isobar separator magnet and also test our tagging technique for future experiments.

To measure the effectiveness of this method for $A = 132$ isobars, we first measured the energy spread as a function of energy loss for pure ^{132}Te beam. The beam was accelerated to 450 MeV and analyzed in the test beamline (see Fig. 1). The results of these measurements are shown in Fig. 8.

The calculated energy spread, predicts very well the measured energy spread of the actual beam when the gas cell is used as an absorber. The first point without any absorber shows a width of 1 MeV (0.2% in energy) attributable to detector timing resolution which in this setup was about 180 ps. The energy spread of the second data point

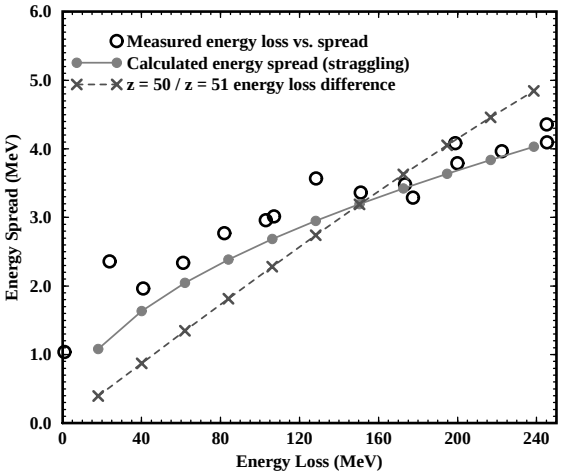

Fig. 8. Measured and calculated energy spread for 450 MeV ^{132}Te passing through the gas cell and the anticipated separation for $z = 51$ and 52 isobars.

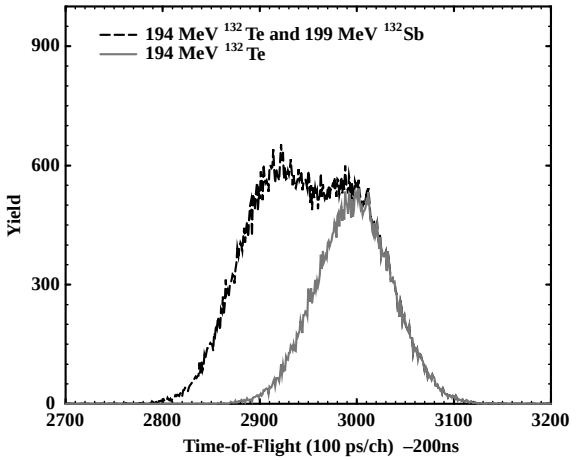

Fig. 9. Simulated TOF spectra for 450 MeV ^{132}Te and ^{132}Sb passing through the gas cell containing 100 Torr isobutane gas.

at 18 MeV energy loss is due to the entrance and exit foil on the gas cell. As repeated measurements with foils alone have shown, the energy spread of particles passing a foil often surpasses what is expected from energy straggling in the foil. This, we assume, is due to inhomogeneities in the foil. Note that the third data point shows a decrease in energy spread. This may be due to the stretching of the foil by the gas filling the cell. Once the magnitude of the energy loss is dominated by losses in the gas absorber, the measurements tend to agree with the predictions of energy spread due to straggling.

From the data in Fig. 8, it is clear that for this case of relatively low energy $A = 132$ isobar mixture we cannot expect complete separation. It was important though to see if the method works at the level predicted and if tagging is a viable option.

We then used the predicted energy losses of different isobars and the measured energy spread as seen in Fig. 8 to simulate the expected separation for ^{132}Te and ^{132}Sb isobars. The results of these simulations are shown in Fig. 9 and confirm that there is substantial overlap but one can attain some degree of isobar separation. These TOF data, when recorded for each event of interest in the reaction, provide an additional variable (tag) associating reaction outcome with differences in isobar mixtures in the beam. Such a spectrum could also provide immediate feedback when one tries alternative beam tuning in order to enhance the yield of one particular isobar.

The beam of $A = 132$ products at rates approaching 1 MHz rate (10^6/s) was then analyzed in our test beamline. Fig. 10 shows several TOF spectra measured for beam particles that passed the gas cell filled with 100 Torr isobutane gas. Several attempts to block out the ^{132}Te component in the beam and modify the ratio of ^{132}Sb and ^{132}Sn were made by modifying the beam tune through the low energy section of the beamline. Fig. 10 shows the result of different current settings in the second stage magnet (isobar separator) in the low energy section. The different TOF spectra show that the isobar mixture can be controlled by tuning the mass separator. The tuned beam, however, still contains a mixture of isobars. By recording the TOF data for events of interest in the experiment, one can select (tag) events from different regions of the TOF spectrum. In this way one could learn about isobaric effects on the reaction of interest. It is also remarkable that we were able to predict the level of ^{132}Sb/^{132}Te separation observed in the experiment.

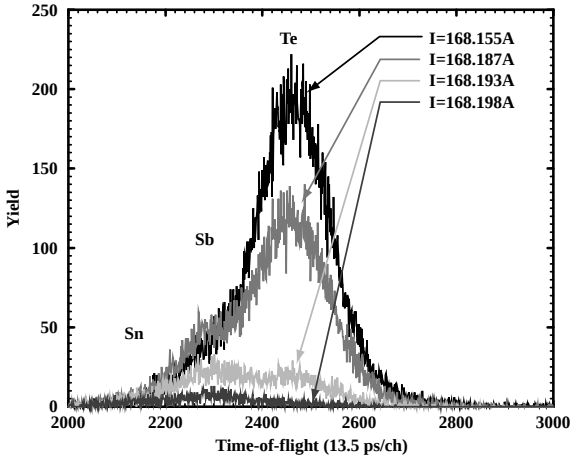

Fig. 10. TOF spectra for a mixture of ^{132}Te, ^{132}Sb and ^{132}Sn with different magnet settings.

5. Conclusions

It is well known that one can separate isobars in a mixed beam by exploiting the difference in energy loss for particles different only in their nuclear charge (z) that pass an absorber. This difference in energy loss can be measured via TOF technique and allows isobar tagging at rates up to 10^7/s or it can be used to select separate isobars with a magnetic separator. This method works best with energetic projectiles because the energy spread due to straggling decreases the closer the ion's charge state is to full stripping. Most important for this method is keeping absorber inhomogeneities to a minimum, and for lower energy ions, the proposed gas cell is one possible method to accomplish this goal. In facilities where projectile fragmentation is used for RIB generation, the available energy will always be sufficient. However, unless isobars can be separated by some other method, it appears that in the design of an ISOL facility for the production of heavy RIBs, allowance must be made for boosting the projectile's energy to allow for isobar separation following energy loss in an absorber.

References

[1] B. Rossi, High Energy Particles, Prentice-Hall, Englewood Cliffs, NJ, 1961, p. 17.
[2] J.F. Ziegler, program SRIM (http://www.research.ibm.-com/ionbeams/\#SRIM).
[3] Program GEANT, PHYS431 (http://wwwinfo.cern.ch/as-doc/geant_html3/node322.html).
[4] G.D. Mills, G.D. Alton, D.L. Haynes, J.R. Beene, Physics Division Progress Report, ORNL-6957, September 1998 (http://www.phy.ornl.gov/progress/hribf/randd/hri031.pdf).
[5] M. Berz, program COSY INFINITY(http://www.beamtheory.nscl.msu.edu/cosy);
M. Berz, Nucl. Instr. and Meth. A 298 (1990) 473.
[6] D. Bardayan, et al., Phys. Rev. Lett. 83 (1999) 45.
[7] J. Gomez Del Campo, et al., Phys. Rev. Lett. 86 (2001) 43.
[8] W. Starzecki, A.M. Stefanini, S. Lunardi, C. Signorini, Nucl. Instr. and Meth. 193 (1982) 499.
[9] H.K. Carter, J. Kormicki, D.W. Stracener, J.B. Breitenbach, J.C. Blackmon, M.S. Smith, D.W. Bardayan, Nucl. Instr. and Meth. B 126 (1997) 166;
(http://www.phy.ornl.gov/hribf/users/beams).